# InAsP quantum dot lasers grown by MOVPE

**Ivan Karomi,[1,4] Peter M. Smowton,[1*] Samuel Shutts,[1] Andrey B. Krysa[2] and Richard Beanland[3]**

[1]*Physics and Astronomy, Queens Building, The Parade, Cardiff, CF24 3AA, UK*
[2]*Department of Electronic and Electrical Engineering, University of Sheffield, S1, UK*
[3]*Department of Physics, University of Warwick, Coventry CV4 7AL, UK*
[4]*University of Mosul, Mosul, Iraq*
[*]*smowtonpm@cardiff.ac.uk*

**Abstract:** We report on InAsP quantum dot lasers grown by MOVPE for 730-780 nm wavelength emission and compare performance with InP dot samples grown under similar conditions and with similar structures. 1-4 mm long, uncoated facet InAsP dot lasers emit between 760 and 775 nm and 2 mm long lasers with uncoated facets have threshold current density of 260 $Acm^{-2}$, compared with 150 $Acm^{-2}$ for InP quantum dot samples, which emit at shorter wavelengths, 715-725 nm. Pulsed lasing is demonstrated for InAsP dots up to 380 K with up to 200 mW output power. Measured absorption spectra indicate the addition of Arsenic to the dots has shifted the available transitions to longer wavelengths but also results in a much larger degree of spectral broadening. These spectra and transmission electron microscopy images indicate that the InAsP dots have a much larger degree of inhomogeneous broadening due to dot size variation, both from layer to layer and within a layer.

OCIS codes: (140.3460) Lasers; (160.4670) Optical materials; (160.4760) Optical properties.

## References and links

1. W.-M. Schulz, M. Eichfelder, R. Roßbach, M. Jetter, and P. Michler, "InP/AlGaInP quantum dot laser emitting at 638 nm," J. Cryst. Growth **315**(1), 123–126 (2011).
2. G. Walter, J. Elkow, N. Holonyak, R. B. Heller, X. B. Zhang, and R. D. Dupuis, "Visible spectrum (645 nm) transverse electric field laser operation of InP quantum dots coupled to tensile strained $In_{0.46}Ga_{0.54}P$ quantum wells," Appl. Phys. Lett. **84**(5), 666–668 (2004).
3. P. M. Smowton, J. Lutti, G. M. Lewis, A. B. Krysa, J. S. Roberts, and P. A. Houston, "InP–GaInP quantum-dot lasers emitting between 690–750 nm," IEEE J. Sel. Top. Quantum Electron. **11**, 103540 (2005).
4. P. J. Schlosser, J. E. Hastie, S. Calvez, A. B. Krysa, and M. D. Dawson, "InP/AlGaInP quantum dot semiconductor disk lasers for CW TEM$_{00}$ emission at 716-755 nm," Opt. Express **17**(24), 21782–21787 (2009).
5. are M. Reischle, C. Kessler, W.-M. Schulz, M. Eichfelder, R. Roßbach, M. Jetter, and P. Michler, "Triggered single-photon emission from electrically excited quantum dots in the red spectral range," Appl. Phys. Lett. **97**(14), 143513 (2010), doi:10.1063/1.3497016.
6. M. Kasim, S. N. Elliott, A. B. Krysa, and P. M. Smowton, "Reducing Thermal Carrier Spreading in InP Quantum Dot Lasers," IEEE J. Sel. Top. Quantum Electron. **21**(6), 1900306 (2015).
7. A. Roggan, M. Friebel, K. Do Rschel, A. Hahn, and G. Mu Ller, "Optical properties of circulating human blood in the wavelength range 400-2500nm," J. Biomed. Opt. **4**(1), 36–46 (1999).
8. A. N. Bashkatov, E. A. Genina, V. I. Kochubey, and V. V. Tuchin, "Optical properties of human skin, subcutaneous and mucous tissues in the wavelength range from 400 to 2000nm," J. Phys. D Appl. Phys. **38**(15), 2543–2555 (2005).
9. M. J. Leahy, "Microvascular blood flow: microcirculation imaging," in *Handbook of Biophotonics* J. Popp, V.V. Tuchin, A. Chiou, and S. Heinemann, eds., Wiley-VCH, Weinheim, Germany ISBN: 978 3–527–41048–4. (2012).
10. H. Wang, L. Kong, A. Forrest, D. Bajek, S. E. Haggett, X. Wang, B. Cui, J. Pan, Y. Ding, and M. A. Cataluna, "Ultrashort pulse generation by semiconductor mode-locked lasers at 760 nm," Opt. Express **22**(21), 25940–25946 (2014).
11. R. Singh, D. Bull, F. P. Dabkowski, E. Clausen, and A. K. Chin, "High power, reliable operation of 730nm AlGaAs laser diodes," Appl. Phys. Lett. **75**(14), 2002–2004 (1999).
12. L. J. Mawsi, S. Rusli, A. Al-Muhanna, and J. K. Wade, "Short wavelength (0.7 μm < λ < 0.78 μm) high power InGaAsP active diode lasers," IEEE J. Sel. Top. Quantum Electron. **5**(3), 785–791 (1999).

13. B. Sumpf, G. Beister, G. Erbert, J. Fricke, A. Knauer, P. Ressel, and G. Trankle, "Reliable 1W CW operation of high-brightness tapered diode lasers at 735nm," IEEE Photonics Technol. Lett. **16**(4), 984–986 (2004).
14. T. W. Schlereth, C. Schneider, S. Gerhard, S. Hufling, and A. Forchel, "Short wavelength (760-920 nm) AlGaInAs Quantum Dot Lasers," IEEE J. Sel. Top. Quantum Electron. **15**(3), 792–798 (2009).
15. Y. Ohba, M. Ishikawa, H. Sugawara, M. Yamamoto, and T. Nakanisi, "Growth of high-quality InGaAlP epilayers by MOCVD using methyl metalorganics and their application to visible semiconductor lasers," J. Cryst. Growth **77**(1-3), 374–379 (1986).
16. H. Hamada, M. Shono, S. Honda, R. Hiroyama, K. Yodoshi, and T. Yamaguchi, "AlGaInP visible laser diodes grown on misoriented substrates," IEEE J. Quantum Electron. **27**(6), 1483–1490 (1991).
17. M. Zorn, H. Wenzel, U. Zeimer, B. Sumpf, G. Erbert, and M. Weyers, "High-power red laser diodes grown by MOVPE," J. Cryst. Growth **298**, 667–671 (2007).
18. S. N. Elliott, P. M. Smowton, A. B. Krysa, and R. Beanland, "The effect of strained confinement layers in InP self-assembled quantum dot material," Semicond. Sci. Technol. **27**(9), 094008 (2012).
19. K. Nishi, H. Saito, S. Sugou, and J.-S. Lee, "A narrow photoluminescence linewidth of 21meV at 1.35mm from strain reduced InAs quantum dots covered by $In_{0.2}Ga_{0.8}As$ grown on GaAs substrates," Appl. Phys. Lett. **74**(8), 1111–1113 (1999).
20. P. Blood, G. M. Lewis, P. M. Smowton, H. D. Summers, J. D. Thomson, and J. Lutti, "Characterisation of Semiconductor Laser gain Media by the Segmented Contact Method," IEEE J. Sel. Top. Quantum Electron. **9**(5), 1275–1282 (2003).
21. P. M. Smowton and P. Blood, "The differential efficiency of quantum-well lasers," IEEE J. Sel. Top. Quantum Electron. **3**(2), 491–498 (1997).
22. J. R. Biard, W. N. Carr, and B. S. Reed, "Analysis of a GaAs laser," Trans. AIME **230**, 286–290 (1964).
23. A. R. Adams, I. P. Marko, N. F. Mass, and S. J. Sweeney, "Effect of non-pinned carrier density above threshold in InAs quantum dot and quantum dash lasers," IET Optoelectron. **8**(2), 88–93 (2014).
24. S. Shutts, P. M. Smowton, and A. B. Krysa, "InP quantum dot lasers with temperature insensitive operating wavelength," Appl. Phys. Lett. **103**(6), 061106 (2013).

# 1. Introduction

InP quantum dots (QD) grown on GaAs substrates have been used as a semiconductor laser active region for output in the 630 – 750nm wavelength range [1–4] and also as single photon sources [5]. Threshold current density, $J_{th}$ can be low in the wavelength range from approximately 680-730 nm with for example a $J_{th}$ of 130Acm$^{-2}$ being achieved for 2mm long, as-cleaved devices at 720nm [6]. However, InP QD laser performance deteriorates for wavelengths longer than 740 nm due to the larger dot size required and/or the less suitable growth conditions e.g. lower growth temperatures as shown in Fig. 6. of [3]. The low $J_{th}$ lasers emitting at shorter wavelengths also have relatively broad gain spectra which support tunable or multi-wavelength sources that can be useful in biophotonic applications. Since longer wavelengths towards 780nm transmit deeper into blood [7], tissue and microvascalature [8] such applications would also benefit from still longer wavelengths. For example in measurements of capillary blood flow [9], longer wavelength measurements from a similar active structure allow measurements at deeper or, with multiple wavelengths, multiple depths. AlGaAs quantum well (QW) based structures have been used to produce mode locked diode laser operation at 760nm for biophotonic applications [10]. Indeed semiconductor lasers incorporating either $Al_xGa_{1-x}As$ QWs [e.g 11.], compressively strained InGaAsP QWs [e.g 12.] or tensile strained GaAsP QWs [e.g 13.] can been used to produce wavelengths in the 720-780nm wavelength range. $Al_xGa_{1-x}As$ based structures tend to be more prone to reliability issues including catastrophic optical degradation at high power densities [11], particularly for high x. InGaAsP structures, optimized for high power operation rather than low threshold current density, have been reported with $J_{th}$ as low as 420Acm$^{-2}$ being achieved for 1 mm long cavities at 730nm and a reduced temperature dependence of threshold current compared to AlGaAs structures [12]. GaAsP QW structures with $J_{th}$ lower than 250 Acm$^{-2}$ with 2 mm long cavities emitting at 735 nm have been reported [13]. Adding aluminium to the usually longer wavelength emitting InGaAs quantum dots to form AlGaInAs quantum dots has produced emission in the 760nm-920nm wavelength range [14].

Here we explore the incorporation of Arsenic in the InP QDs as a means to produce longer wavelength laser emission while still maintaining relatively low threshold currents and in a

structure compatible with the use of InP quantum dots in additional layers to, in future structures, also cover shorter wavelength emission.

## 2. Growth structure

The structures, which are represented in Fig. 1, are produced with a relatively standard MOVPE process [15–17] for manufacturing AlGaInP-based red lasers, including commonly used group V precursors, arsine and phosphine for the InAsP QD growth.
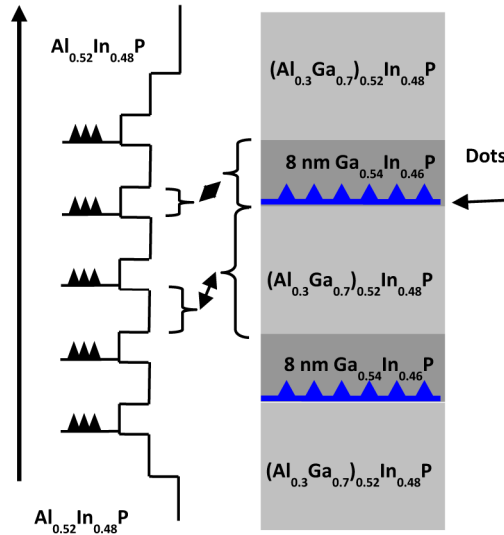


Fig. 1. Schema of epitaxial growth structure.

Reference InP QD laser structures, which are of a similar designs to those discussed in [18] are also grown for comparison. The active region of the laser structures consisted of 5 InP or InAsP QD sheets with a $Ga_{0.54}In_{0.46}P$ quantum well with a thickness of 8 nm grown above each QD sheet and separated by a layer of $(Al_{0.3}Ga_{0.7})_{0.52}In_{0.48}P$ with a thickness of 16 nm. The intended role of the $Ga_{0.54}In_{0.46}P$ layer above the dots is similar to the D-Well of InGaAs in the InAs dot system, where it helps maintain the height of the dots [19] and acts as a carrier reservoir with additional benefits for InP dots detailed in [18]. The phosphine flow was kept constant at 300 sccm throughout the growth of the core regions, and the arsine flow of 6.25 sscm was introduced to the reactor during the growth of InAsP QD layers. Based on θ-2θ X-ray diffraction scans near 004 of bulk $InAs_xP_{1-x}$ grown with the same growth conditions as the InAsP QDs, we would expect a solid molar fraction of arsenic of around 25%. Such a proportion of As would be expected to produce an increase in emission wavelength of approximately 120 nm (~250meV) compared to InP bulk material. The active region was sandwiched with an $Al_{0.52}In_{0.48}P$ clad / $(Al_{0.3}Ga_{0.7})_{0.52}In_{0.48}P$ core waveguide.

Transmission electron microscope (TEM) images were taken of these samples and representative images are shown in Fig. 2. While not providing sufficient sampling for a statistical evaluation, the TEM images show no evidence for a difference in dot density, being of the order of $10^9 – 10^{10}$ cm$^{-2}$ for both samples. The dot density was calculated by counting their number in a length of cross section TEM specimen, converted into an areal density using an estimate of the specimen thickness obtained by tilting by 15 degrees about the [-110] axis and measuring the projected width of (001) interfacial or surface planes.
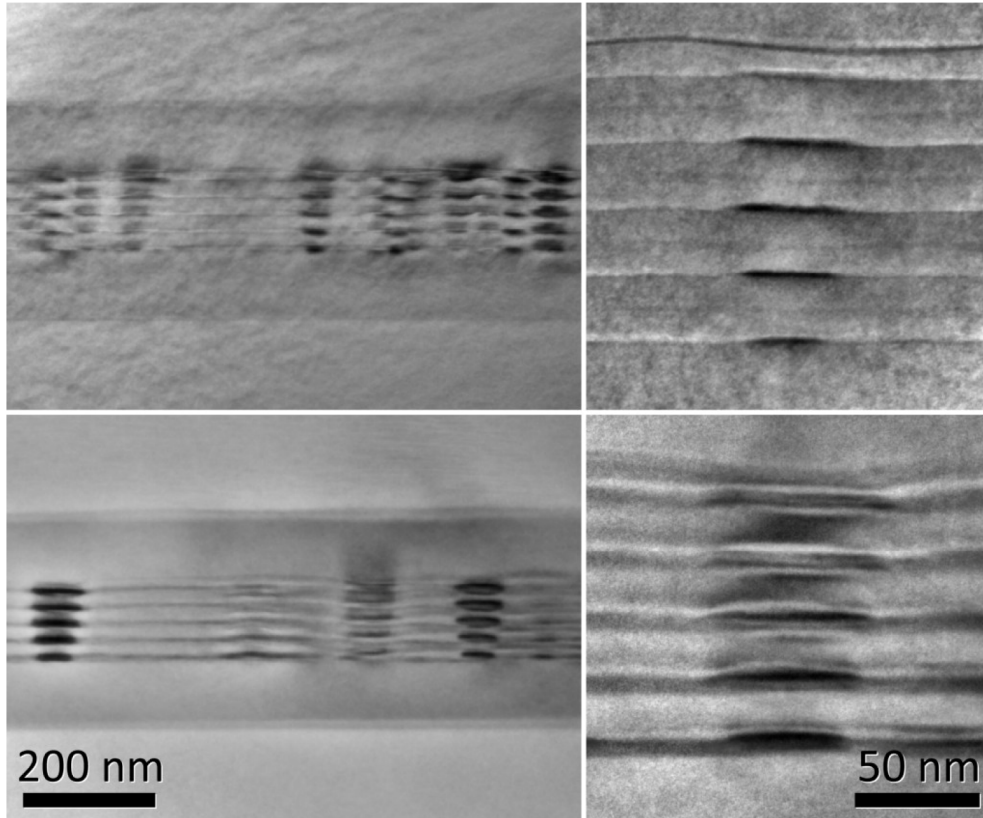
Fig. 2. Transmission electron microscope images of 5 layers of InAsP dots (upper) and InP dots (lower). Left: bright field, **g** = 004 image showing several stacks of dots; right: dark field, **g** = 002, showing the changes in dot size and shape for an individual stack.

For both structures the dots in different layers are aligned in isolated vertical stacks. Although there is considerable variation from stack to stack, the bottom layer usually contains the smallest dots, with a diameter of a few tens of nm; often, the diameter gradually increases through the stack until the dots in the top layer have roughly twice that of those at the bottom, while the height is unchanged. The InP dots generally appear larger and the stacks more regular than the InAsP dots, with a height of 4-5 nm and a lowermost dot diameter of 40-50 nm, whereas the InAsP dots have a height of 2-3 nm, a lowermost dot diameter of 20-30 nm and greater variability in dot diameter through the stack. It is not yet clear whether the smaller dot size and greater size variation is a fundamental property of the InAsP dots (e.g. due to a higher lattice mismatch) or simply results from using growth conditions optimised for InP dots, which may not be optimal for the InAsP dots. Photoluminescence (PL) measurements taken at room temperature using a Biorad PL mapper with a 532 nm excitation laser are shown in Fig. 3. While the width of the PL spectrum is dependent on the carrier density within the sample, which depends on both the collected pump power, which was nominally the same, and the non-radiative recombination rates these results do indicate both an increased broadening of the InAsP dot material spectrum and a shift to longer emission wavelengths.
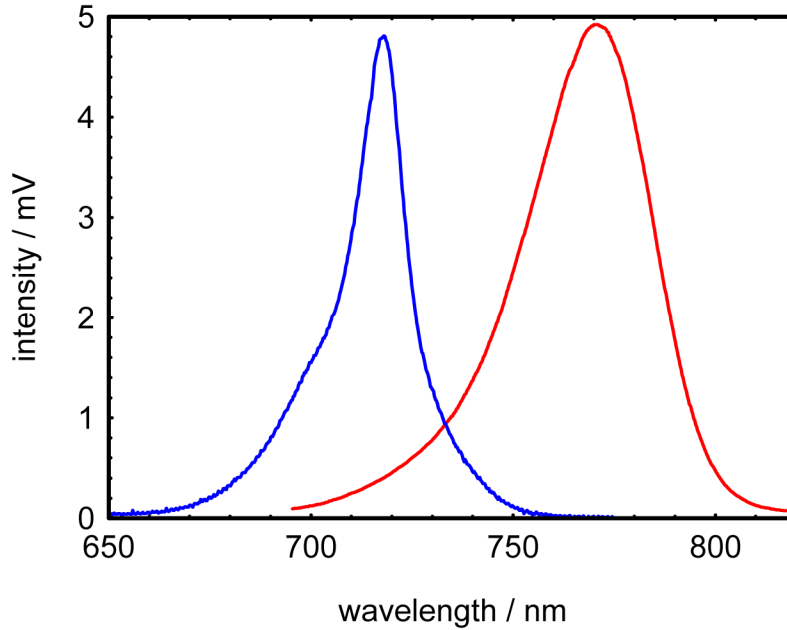
Fig. 3. Photoluminescence measurements taken at room temperature with an excitation wavelength of 532 nm. Data for the InP dot material in blue and the InAsP dot material in red (longer wavelength broader spectrum).

## 3. Fabrication

Broad area (50 μm wide) oxide-isolated stripe lasers and test structures were fabricated to allow laser characterization and measurement of absorption and gain spectra using the segmented contact method [20]. Lasers of length 1, 2, 3 and 4 mm are made with uncoated facets and mounted for pulsed operation.

## 4. Laser results

Lasers were tested in pulsed operation, with a repetition rate of 1 kHz and a pulse width of 1 μs to avoid self-heating effects. The room temperature power-current (P-I) characteristics (shown in Fig. 4) of 1 and 4 mm long lasers with as-cleaved facets were measured using an integrating sphere to output peak pulse powers beyond 200 mW and to the limit of our current driver without any sign of rollover. The threshold currents are larger for the InAsP QD lasers, and the slope efficiencies are poorer for the same length cavities. The slope efficiency is related to the internal optical mode loss, $\alpha_i$ and the internal differential efficiency, $\eta_i^d$, through the relation:

$$\frac{dP}{dI} = \frac{hf}{e}\eta_i^d \frac{\ln \frac{1}{R}}{\alpha_i L + \ln \frac{1}{R}},$$

where the $d$ subscript indicates a differential or slope value derived above threshold [21], $hf$ is the photon energy, $e$ the electronic charge, $R$ the mirror reflectivity and $L$ the cavity length.
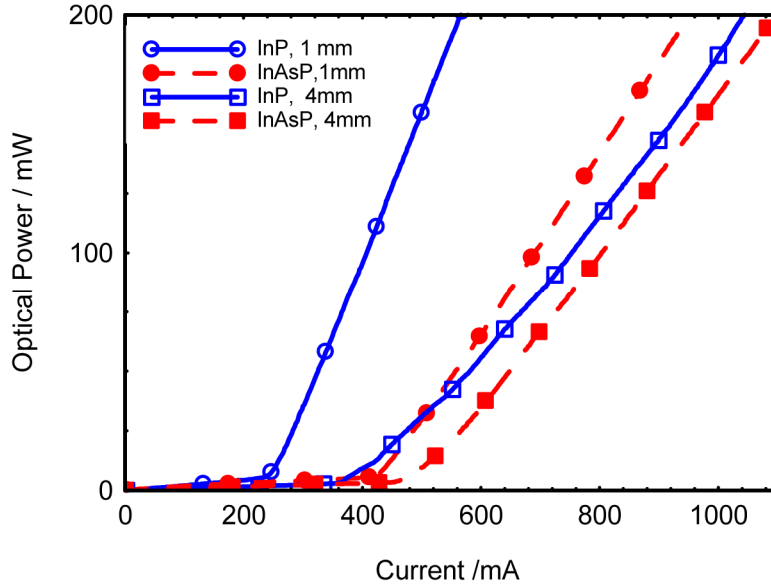
Fig. 4. Pulse peak power-current characteristic for InP (blue with open symbols) and InAsP (red with closed symbols) for 1 (circles) and 4 (squares) mm long lasers taken at 300 K in pulsed operation.
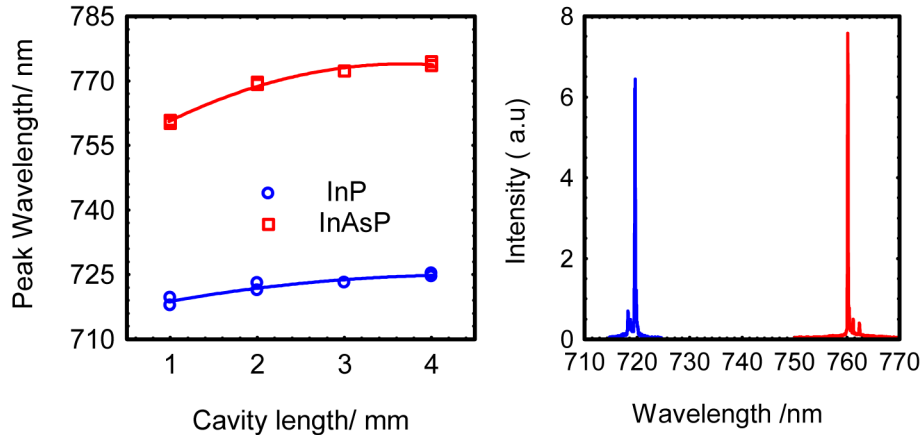


Fig. 5. a) Lasing wavelength for InP and InAsP dot samples for 1, 2, 3 and 4 mm long lasers in pulsed operation and b) example spectra for 1 mm long lasers.

This is often used to determine the values of $\alpha_i$ and $\eta_i^d$ from the measured slopes. Here this is inappropriate because the slope is varying with current and presumably device length for some of the device lengths and a constant $\eta_i^d$ is an assumption of the analysis [21, 22]. Furthermore using the measured value of internal optical mode loss (see later) and calculated mirror loss and the slopes derived from Fig. 4 indicate an internal differential efficiency of approximately 25%. This is much less than the values typically obtained from broad area oxide isolated stripe lasers and suggest that mechanisms such as incomplete carrier pinning, which is well known in QD lasers [23] are limiting the slope via $\eta_i^d$ rather than being limited by the values of $\alpha_i$ and R. The lasing wavelength, measured at 1.1 times threshold current for each laser, is plotted as a function of the device length and example spectra are shown in Fig. 5. The emission wavelength varies between 760 and 775 nm for the InAsP dot lasers as compared with 715-725 nm for the InP dots. This difference of 45-50 nm (103-110 meV) is

much smaller than the difference expected due to an arsenic incorporation of 25% but demonstrates that longer wavelength lasers can be produced while maintaining reasonable threshold currents and power outputs. The larger range of lasing wavelengths obtained with cavity lengths between 1 and 4 mm may be a sign of greater gain saturation in the InAsP dot material and will be discussed later.

More detailed measurements of threshold current density as a function of heat sink temperature, some of which are plotted in Fig. 6, confirm that the threshold current density is larger for the InAsP material, although this difference decreases for longer device length. The threshold of the longer device lengths is slightly less temperature dependent for the InAsP as compared to the InP dot samples as quantified using the much used $T_0$ parameter where for example $T_0$ (measured between 300 and 400K) increases from 60 to 65K for the 2mm long InP and InAsP samples respectively. However, $T_0$ is not a perfect way to quantify temperature dependence as it also depends on the magnitude of the threshold current density and the more important fact is that operation up to at least 380 K is readily achieved for both materials. The rapid increase in threshold current density with temperature at high temperatures in the InP dot lasers is thought to be due to the thermally activated loss of carriers from the dots [6]. InAsP dots with a deeper confining potential would be expected to have less thermally activated loss and a slower rate of increase of threshold for a similar Fermi level separation.
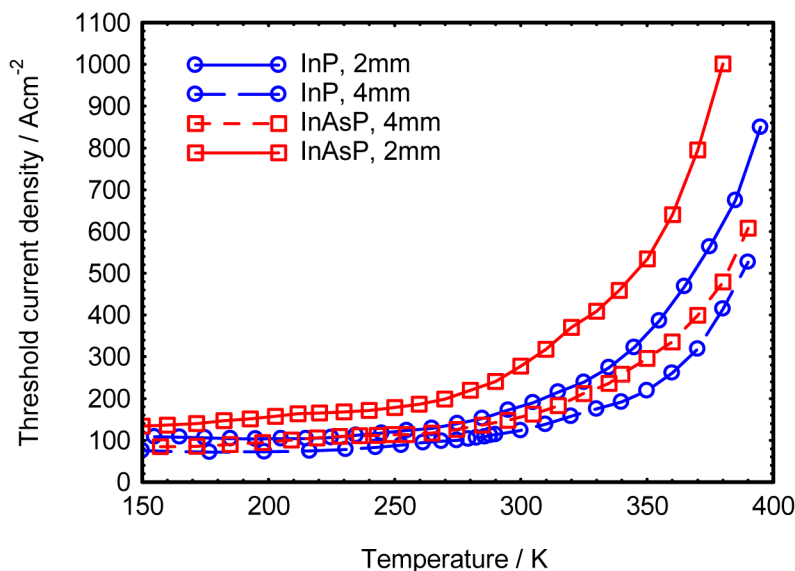


Fig. 6. Threshold current density for 2 and 4 mm long lasers as a function of heat-sink temperature.

To understand the origin of the slightly higher threshold current density of the InAsP dot samples we measure the modal absorption using the segmented contact technique [18]. The modal absorption is a function of the transitions between states available in the material when the material is unpumped and therefore reflects how the states in the system have changed between InP and InAsP material. The results, shown in Fig. 7, indicate that as expected, the InAsP spectra are shifted to longer wavelength, albeit by less than the 120nm that would be expected for 25% As incorporation, but they are also significantly broader than the InP dot spectra. This broadening is consistent with the increased variation in dot size seen in the TEM micrographs. The smaller than expected lengthening of the wavelength may also be consistent with the smaller InAsP dots observed in the TEM images, which shortens the wavelength due to the enhanced quantum size effect relative to the InP dots. The absorption spectrum is appreciably broader and the amplitude at the ground state is significantly reduced, which may

result in less gain being available from the ground state, when carriers are present. The increase in absorption for the InAsP sample at short wavelengths near 660 nm is the onset of absorption from the $Ga_{0.54}In_{0.46}P$ quantum well, which is also present for the InP sample although not shown here. The internal optical mode loss ($\alpha_i$) was extracted from the segmented contact data [20] indicating values of $3.2 \pm 1.5$ cm$^{-1}$ for InP and $4.5 \pm 1.8$ cm$^{-1}$ for InAsP samples.
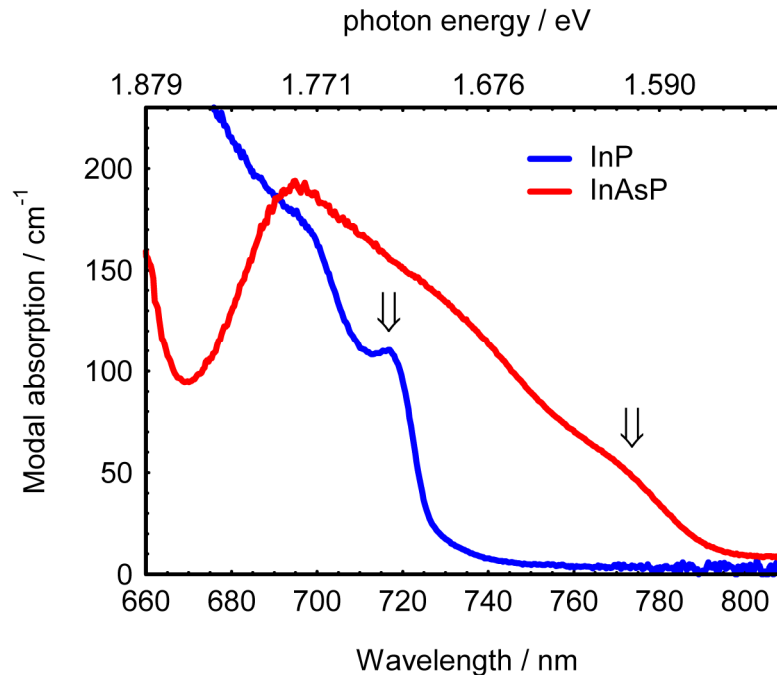
photon energy / eV



Fig. 7. Measured modal absorption spectra for InP and InAsP dot samples. The the absorption arising from the inhomogenously broadened dot ground state is indicated by an arrow for both the InP and InAsP dots spectra.

Optical gain spectra are also measured using the segmented contact method and are plotted in Fig. 8. The gain shown arises entirely from the quantum dots with the tensile strained $Ga_{0.54}In_{0.46}P$ quantum well having a bandgap of 1.93eV. The InAsP gain spectra, while shifted to longer wavelength, are only slightly broader than the InP dot spectra and do require more current to achieve the same peak gain. The energy of the peak of the gain spectra does increase (wavelength decrease) more quickly with increasing current density and gain magnitude for the InAsP dots as is consistent with the observation of change in lasing wavelength with device length in Fig. 5. This change in gain peak wavelength with increasing current in InP quantum dot lasers has been observed to be largest where the gain magnitude is saturating with increasing current and attributed to the thermal state filling of a relatively flat energy distribution of dot states [24]. The absorption spectra of Fig. 7 do demonstrate a reflectively flatter distribution of state transitions for the InAsP system compared to the InP dots. The larger gain saturation in the InAsP dot lasers is further emphasized by plotting the gain peak magnitude from each of the spectra of Fig. 8 versus current density in Fig. 9.
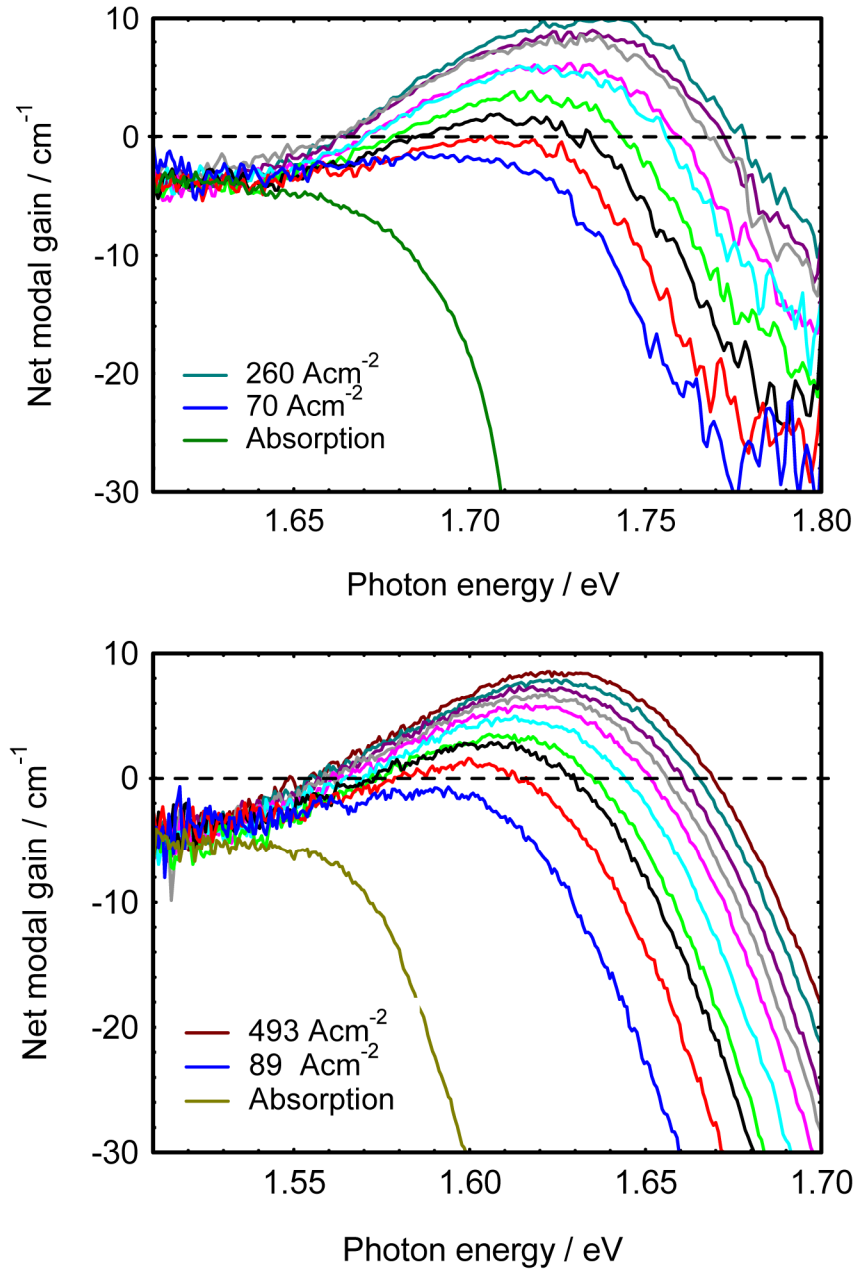
Fig. 8. Measured modal gain spectra for InP (upper) and InAsP (lower) dot samples. Note the difference in the x-axes, where the magnitude of the energy range is the same but the start and end points differ to illustrate the shift seen.
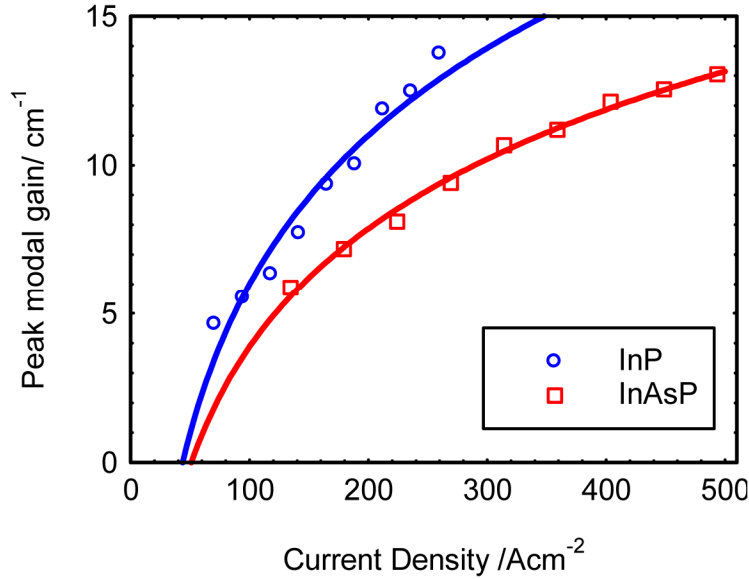
Fig. 9. Measured peak modal gain versus current density

## 5. Conclusions

In summary, we have grown, fabricated and characterized InAsP QD laser material and have found that longer wavelength emission out to almost 780 nm is possible with this material while maintaining a useable threshold current density (increase of 110 $Acm^{-2}$ compared to a reference InP structure for 2 mm device lengths at room temperature). Peak power in the pulse above 200 mW is achieved with a negligible reduction in slope efficiency compared to the InP reference structure. Growth was carried out under conditions appropriate for InP dots and the relatively small increase in threshold current density of the InAsP dot lasers may be improved following growth optimization, such as changing the growth temperature of the dot and adjacent layers for the InAsP dots. These results also open the possibility of growing both InP and InAsP dots in the same structure creating very broadband or widely tunable sources.

## Acknowledgments